Inorganic Chemistry

Article

pubs.acs.org/IC

Lanthanide Metal–Organic Frameworks: Searching for Efficient Solvent-Free Catalysts

Richard F. D'Vries, Marta Iglesias, Natalia Snejko, Enrique Gutiérrez-Puebla, and M. Angeles Monge*

Instituto de Ciencia de Materiales de Madrid (ICMM-CSIC), Cantoblanco, 28049 Madrid, Spain

Supporting Information

ABSTRACT: Three Ln-based 2D metal–organic frameworks with the formula [Ln(3,5-DSB)(Phen)] (Ln = La, Pr, Nd; 3,5-DSB = 3,5-disulfobenzoate; Phen = 1,10-phenanthroline) were hydrothermally synthesized. They belong to two 2D structural types, and their nets own different topologies. The isostructural La and Pr compounds possess a uninodal 5-connected SP 2-periodic net (6,3). The Nd compound has a binodal 3- and 6-connected kgd net. The novel compounds exhibit excellent catalytic activities toward the cyanosilylation reaction under solvent-free conditions.

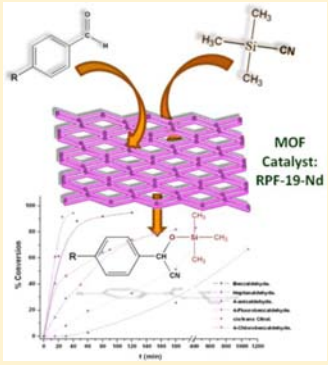

INTRODUCTION

Nowadays, the particular field of materials science related to metal–organic frameworks (MOFs) or coordination polymers (CPs) is being extensively studied, mainly because of the well-known multiple properties of these materials.[1] Especially interesting are those connected with heterogeneous catalysis.[2] The "design"[3] and fine characterization of these compounds is fundamental to defining the possible catalytic properties and corresponding activity. Within the "design", the selection of the metal center, ligand, and/or ancillary ligand can direct the dimensionality, topology, and accessibility to the active center.[4]

Our interest being focused on lanthanide cations has allowed us the assembly of new structures with catalytic activity toward sulfide oxidation,[1c,5] aldehyde acetalization,[6] olefin epoxidation,[7] hydrogenation,[8] and cyanosilylation reactions.[9] Furthermore, the use of sulfonate ligands as multitopic linkers led us to find a good number of different architectures and topologies.[1e]

Sulfonate ligands are considered to be poor electron donors and weak coordinative ligands,[10] but under certain hydrothermal or solvothermal conditions, coordination to the metallic centers, especially to lanthanide cations, is favored. As a way to control the polymeric compound net dimensionality, the use of ancillary blocking ligands, for example, chelate nitrogen molecules, is in some cases very useful.

In this work, three new hydrothermally synthesized MOF materials with the formula [Ln(3,5-DSB)(Phen)] (Ln = La, Pr, Nd; 3,5-DSB = 3,5-disulfobenzoic acid; Phen = 1,10-phenathroline) are presented. Their structural and topological studies and complete characterization, as well as their catalytic properties, are also described.

The bidimensional nets present two different topologies given by the coordination modes of the sulfonate group. We demonstrate that these catalysts are very efficient in the cyanosilylation of carbonyl compounds and allow the reaction to be carried out under solvent-free conditions using only a low loading of the catalyst, which can be recovered and reused without displaying any significant loss of activity.

EXPERIMENTAL SECTION

General Information. All reagents and solvents employed were commercially available and were used as supplied without further purification: 3,5-disulfobenzoic acid, disodium salt (98% Sigma-Aldrich); 1,10-phenanthroline (99% Sigma-Aldrich); praseodymium nitrate hexahydrate (99.9% Strem Chemicals); neodymium nitrate hexahydrate (99.9% Alfa Aesar); lanthanum nitrate hexahydrate (99.9% Alfa Aesar).

The IR spectra were recorded from KBr pellets in the range 4000–250 cm^{-1} on a Bruker IFS 66 V/S spectrometer. Thermogravimetric and differential thermal analyses (TGA/DTA) were performed using a Seiko TGA/DTA 320U analyzer in a temperature range between 25 and 1000 °C in an air atmosphere (100 mL/min flow) with a heating rate of 10 °C/min. A Perkin-Elmer CNHS analyzer 2400 was employed for elemental analysis.

Synthesis. [Ln(3,5-DSB)(Phen)] (Ln = Pr, La; **RPF-18**, which is a rare-earth polymer framework) and [Nd(3,5-DSB)(Phen)] (**RPF-19**) were synthesized (Scheme 1) by the addition of 3,5-$DSBNa_2$ (0.0375 g, 0.115 mmol) and phenanthroline (0.036 g, 0.2 mmol) to a solution of $Ln(NO_3)_3{\cdot}6H_2O$ (0.05 g, 0.115 mmol) in water (6 mL); the resultant reaction mixture was magnetically stirred at room temperature for 15 min, placed in a Teflon-lined stainless steel autoclave, and heated at 200 °C for 3 days. After cooling to room temperature, the crystalline products were filtered and washed with water and acetone with a yield of 71.3, 65.2, and 69.7% for Pr, La, and Nd, respectively. Elem anal. Calcd for the Pr compound ($C_{19}H_{11}N_2O_8S_2Pr$): C, 37.98;

Received: April 20, 2012
Published: October 22, 2012

   dx.doi.org/10.1021/ic300816r | *Inorg. Chem.* 2012, 51, 11349–11355

Scheme 1. Representations of the Coordination Modes for the 3,5-DSB Ligand

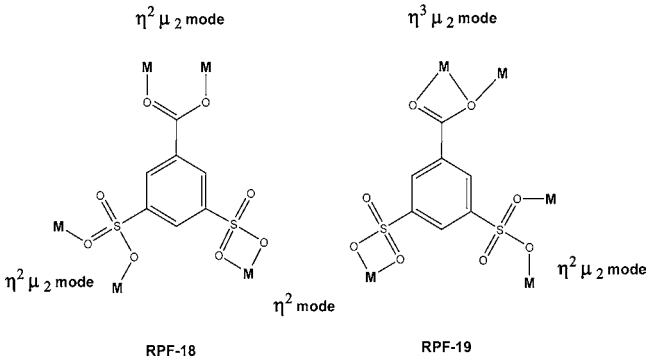

H, 1.83; S, 10.66; N, 4.66. Found: C, 37.73; H, 1.77; S, 10.12; N, 4.09. Calcd for the La compound ($C_{19}H_{11}N_2O_8S_2La$): C, 38.10; H, 1.84; S, 10.70; N, 4.68. Found: C, 37.30; H, 1.88; S, 9.24; N, 4.57. Calcd for the Nd compound ($C_{19}H_{11}N_2O_8S_2Nd$): C, 37.77; H, 1.82; S, 10.60; N, 4.64. Found: C, 37.80; H, 1.88; S, 10.05; N, 4.59.

Single-Crystal Structure Determination. Single-crystal X-ray data for all of the compounds were obtained in a Bruker-Siemens Smart CCD diffractometer equipped with a normal-focus, 2.4-kW sealed-tube X-ray source (Mo Kα radiation = 0.71073 Å) operating at 50 kV and 30 mA. Data were collected over a hemisphere of the reciprocal space by a combination of three sets of exposure. Each exposure of 20 s covered 0.3° in ω. The unit cell dimensions were determined for a least-squares fit of reflections with $I > 20\sigma$. The structures were solved by direct methods. The final cycles of refinement were carried out by full-matrix least-squares analyses with anisotropic thermal parameters of all non-hydrogen atoms. The hydrogen atoms were fixed at their calculated positions using distance and angle constraints. All calculations were performed using *SMART* software for data collection,[11] *SAINT* for data reduction,[12] and *SHELXTL* to solve and refine the structure.[13]

Powder X-ray Diffraction (PXRD). PXRD patterns were measured with a Bruker D8 diffractometer, with step size = 0.02° and exposure time = 0.5 s/step. PXRD measurements were used to check the purity of the obtained microcrystalline products by a comparison of the experimental results with the simulated patterns obtained from single-crystal X-ray diffraction data. The residues of the compounds after TGA were analyzed by PXRD and compared with inorganic crystal structure database (ICSD) patterns reported.

CATALYTIC STUDY

Cyanosilylation. The detailed reaction conditions are shown in the captions of Table 1 and Scheme 2. A typical procedure for cyanosilylation of carbonyl compounds is as follows: Into a Pyrex-glass screw-cap vial (volume: ca. 10 mL) was successively placed 10 mg (5 mol %) of benzaldehyde (0.33 mmol) in the absence of solvent. A Teflon-coated magnetic stirbar was added, and the reaction was initiated by the addition of trimethylsilyl cyanide (TMSCN; 0.495 mmol). The reaction mixture was vigorously stirred (800 rpm) at 50 °C under a N_2 atmosphere. The conversion of benzaldehyde and the product yield were periodically determined by gas chromatography (GC) analysis. After the reaction was completed, the catalyst was removed by filtration and centrifugation of the reaction mixture. All products (cyanohydrin trimethylsilyl ethers) were confirmed by a comparison of their GC retention times, GC–MS spectra, and/or ^{1}H and ^{13}C NMR spectra with those of authentic data. GC analysis was performed using a Konik HRGC 4000B gas chromatograph–mass spectreometer and cross-linked 95% dimethyl–5% diphenylpolysiloxane (Teknokroma TRB-5MS) column of 30 m length.

Table 1. Scope of Ln-MOF-Catalyzed Cyanosilylation of Aldehydes

Compound	Aldehyde	Time (h)	Yield (%)[a]	TOF (h^{-1})[b]
RPF-18-Pr	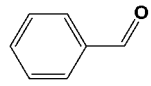	3	77.8	6.48
RPF-18-La		2	85.7	9.38
RPF-19-Nd		2	94.8	12.94
	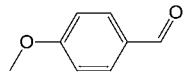	18	66.8	13
	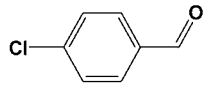	3	81.9	21.7
RPF-19-Nd (1%)	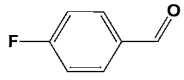	2.5	79.2	40.5
	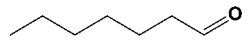	0.75	94.3	243.9
	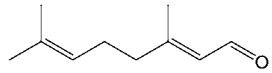 *cis / trans*	7	83.2 47.4 /52.6	18.5
Blank[c]	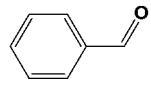	6	64.7	

[a]Yield determined by GC–MS. [b]TOF: % conversion (mmol of substrate/mmol of cat. h). [c]0.33 mmol of benzaldehyde; 0.5 mmol of TMSCN; 50 °C.

Scheme 2. Cyanosilylation of Aldehydes with TMSCN[a]

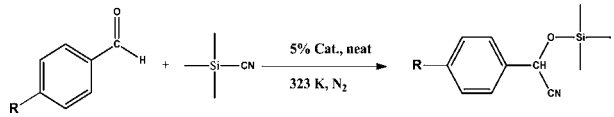

[a]Reaction conditions: catalyst (5 mol %), benzaldehyde (0.5 mol), TMSCN (molar ratio TMSCN:benzaldehyde = 1:1.5), without solvent, 50 °C, 2 h.

Recycle Experiment. The recycle experiment was carried out for cyanosilylation of benzaldehyde. The reaction was carried out under standard conditions. After the reaction was completed (more than 95% conversion, 120 min), the catalyst was recovered by filtration (7.7 mg, 77% recovery), washed with acetone, and air-dried prior to being used for the recycle experiment. The PXRD pattern of the retrieved catalyst was identical with that of the fresh caltalyst (Figure S6 in the Supporting Information). In addition, the recovered catalyst can be reused for cyanosilylation of benzaldehyde without an appreciable loss of its high catalytic performance. When cyanosilylation of benzaldehyde was carried out with the recovered catalyst under standard conditions, cyanohydrin was obtained in 92% yield (120 min).

dx.doi.org/10.1021/ic300816r | *Inorg. Chem.* 2012, 51, 11349–11355

Table 2. Crystal and Refinement Data for Compounds RPF-18-La, Pr, and RPF-19-Nd[a,b]

	RPF-18-La	RPF-18-Pr	RPF-19-Nd
empirical formula	$C_{19}H_{11}N_2O_8S_2La$	$C_{19}H_{11}N_2O_8S_2Pr$	$C_{19}H_{11}N_2O_8S_2Nd$
fw	598.35	600.35	603.68
temperature (K)	298(2)	298(2)	298(2)
wavelength (Å)	0.71073	0.71073	0.71073
cryst syst	monoclinic	monoclinic	monoclinic
space group	*C*2/*c*	*C*2/*c*	*P*2(1)/*c*
unit cell dimens			
a (Å)	13.9971(16)	13.9344(8)	14.3054(14)
b (Å)	11.3873(13)	11.3010(7)	11.1468(11)
c (Å)	24.372(3)	24.2873(15)	12.5648(13)
α (deg)	90	90	90
β (deg)	97.031(2)	97.1830(10)	101.059(2)
γ (deg)	90	90	90
V (Å^3)	3855.4(8)	3794.6(4)	1966.4(3)
Z	8	8	4
ρ_{calc} (mg/m^3)	2.062	2.102	2.039
abs coeff (mm^{-1})	2.488	2.844	2.907
F(000)	2336	2352	1180
θ range for data collection (deg)	2.31−26.38	1.69−26.37	2.33−25.03
reflns collected/unique [*R*(int)]	14772/3897 [0.0683]	14674/3863 [0.1124]	13875/3449 [0.0512]
completeness (%)	98.5	99.6	99.2
data/restraints/param	3897/0/289	3863/0/271	3449/0/289
GOF on F^2	1.142	1.189	1.076
R1 [$I > 2\sigma(I)$]	0.0583	0.0897	0.0340
wR2 [$I > 2\sigma(I)$]	0.0971	0.1974	0.0547
R1 (all data)	0.0845	0.1153	0.0523
wR2 (all data)	0.1037	0.2148	0.0582
largest diff peak and hole (e/A^3)	0.770 and −2.289	2.890 and −2.840	0.733 and −0.660

[a]Absorption correction: semiempirical from equivalents. [b]Refinement method: full-matrix least squares on F^2 in all cases.

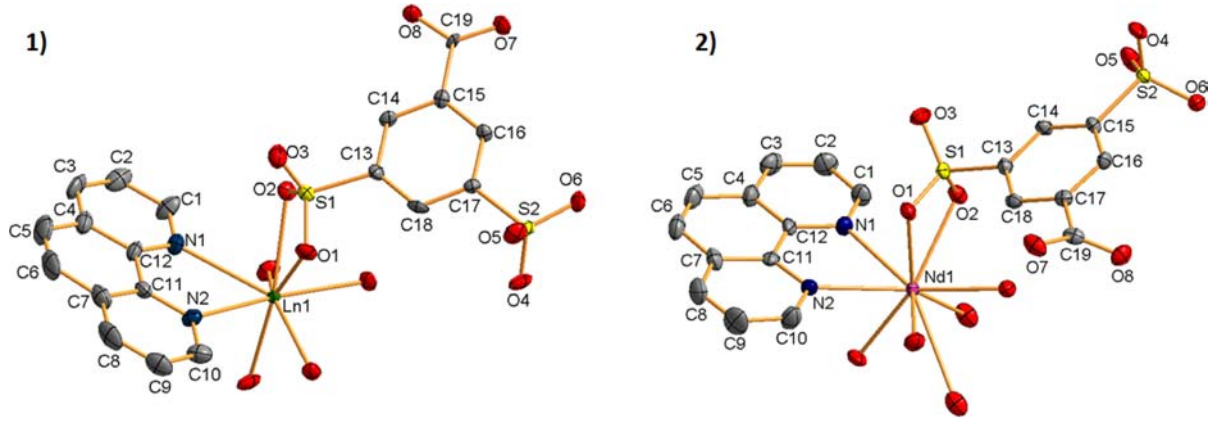

Figure 1. ORTEP drawings of the asymmetric units for (1) **RPF-18-Ln** (Ln = La, Pr) and (2) **RPF-19-Nd**. Ellipsoids are displayed at the 50% probability level.

RESULTS AND DISCUSSION

Structural Description. The details of data collection, refinement, and crystallographic data are summarized in Table 2, and ORTEP drawings are present in Figure 1.

[Ln(3,5-DSB)(Phen)] (Ln = Pr, La) compounds are isostructural and belong to the **RPF-18** type; they crystallize in the monoclinic space group *C*2/*c*. The trivalent cation is at the center of a trigonal-prismatic square-faced bicapped polyhedral (TPRS-8)[14] formed by two nitrogen atoms of a phenanthroline molecule, as a chelate blocking ligand, four sulfonates, and two carboxylate oxygen atoms [LnN_2O_6]. The carboxylic and one of the sulfonic groups are bridging two cations in a $\eta^2\mu_2$ mode, while the other sulfonic group is bonded to the cation in a η^2 mode (Figure 2).

Polyhedra are alternatively linked through sulfonate and carboxylate bridges, giving rise to inorganic chains along the [100] direction, which can be considered as inorganic secondary building units (SBUs). Distances Ln−(*μ*-carboxylate)−Ln are 5.7228(7) and 5.6724(10) Å, and Ln−(*μ*-sulfonate)−Ln are 6.2812(7) and 6.2442(9) Å for Pr and La, respectively. Junctions of these chains through the whole 3,5-DSB organic anion create layers in the plane (110), with the phenantroline ligand pointing out of them (Figure 3b).

dx.doi.org/10.1021/ic300816r | *Inorg. Chem.* 2012, 51, 11349−11355

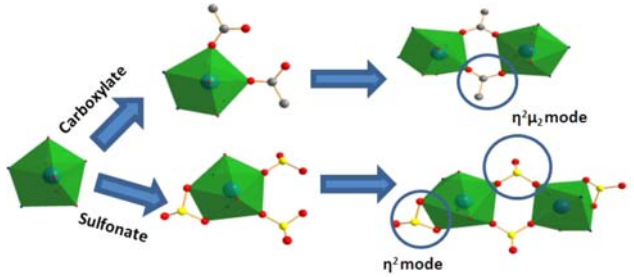

Figure 2. Polyhedron representation and bridge formation by the sulfonate and carboxylate groups in **RPF-18**.

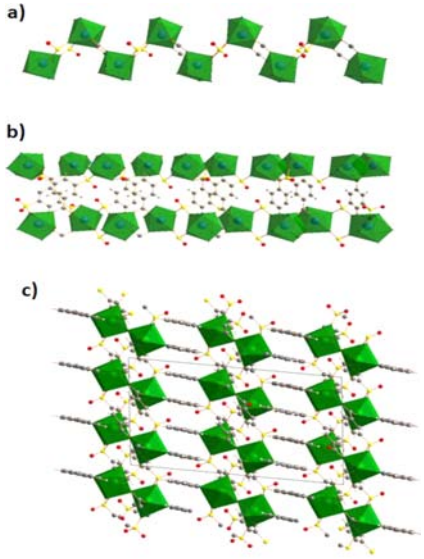

Figure 3. RPF-18 representation of (a) chains along [100], (b) layer formation through ligand connection, and (c) view of the 3D supramolecular structure along [010].

Therefore, layer pillaring gives rise to $\pi-\pi$-stacking interaction along the [001] direction, with distances between centroids of 3.758(2) and 3.784(3) Å and dihedral angles of 1.14(4) and 1.68(3)° for **RPF-18-Pr** and **RPF-18-La**, respectively. These arrangements allow formation of the $\pi-\pi$-stacking 3D supramolecular structure (Figure 3c).

Topological analysis reveals that **RPF-18** owns a 2D uninodal net, in which both the metallic centers and the ligands act as 5-connected nodes. By considering the phenanthroline molecule and the η^2 sulfonate as 0- and 1-connected ligands, respectively, the $[LnN_2O_6]$ polyhedra become 5-connected nodes. The other 5-connected nodes are taken in the aromatic ring centroids and connect five metallic cations (Figure 4). This topology has a point (Schläfli) symbol $(4^8.6^2)$, and it was considered to be a SP 2-periodic net (6,3)IIa in the 1D-2D.TTD database.[15]

RPF-19, [Nd(3,5-DSB)(Phen)], with the same stoichiometry as that of **RPF-18** and quite similar environment around the metallic center, owns different structures and topological nets. The Nd cation is surrounded by the chelating phenanthroline molecule and seven different oxygen atoms, giving rise to original $Nd_2N_4O_{12}$ edge-sharing dimeric units. Besides the $\eta^3\mu_2$ oxo–carboxylate bond, responsible for the dimeric SBU formation, the two polyhedra are also bonded via two sulfonate bridges. Every Nd polyhedron can be thought as a trigonal-prismatic square-faced tricapped one (TPRS-9). The

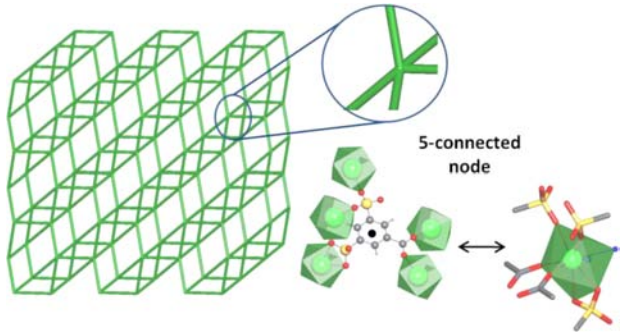

Figure 4. Schematic description of the SP 2-periodic net (6,3)IIa in **RPF-18**.

3,5-DSB ligand acts as $\eta^3\mu_2$ (CO_2^-), $\eta^2\mu_2$, and η^2 (SO_3^-) heptatopic ligands. This arrangement gives rise to a 2D structure, with the layers perpendicular to the [100] direction. Like in **RPF-18**, the phenanthroline molecules are interdigitated, pointing toward the interlamellar space. The $\pi-\pi$-stacking interactions are weaker than those in the former structural type, and as the phenanthroline molecules are shifted toward each other, interactions only remain between every two phenanthroline external rings [centroid distance 3.6889(2) Å]. The 3D supramolecular net along the [001] direction is depicted in Figure 5.

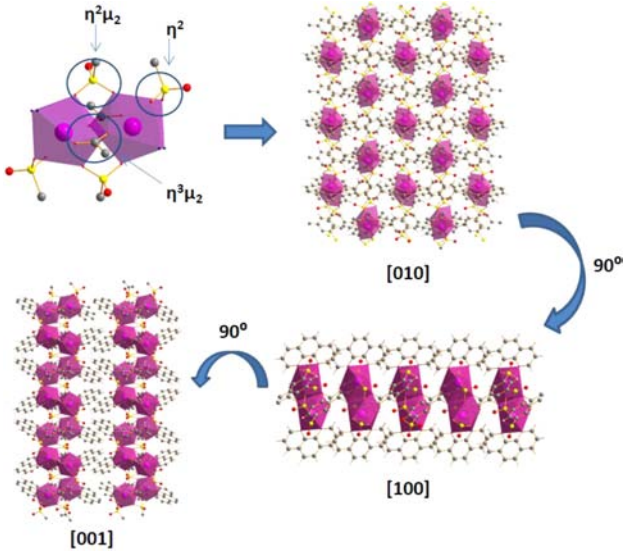

Figure 5. RPF-19 schematic representation of the coordination modes of the sulfonate and carboxylate in the dimerc unit and views of the structure in the directions [100], [010], and [001].

The net simplification for the topological study was done as follows: One nodal point was fixed in the middle of the $Ln_2O_{12}N_4$ SBU, and the SBU links six ligand molecules (the 0-connected Phen is not taken into account) and, therefore, can be considered as a 6-connected node. On the other hand, the ligand links three dimeric units (SBUs), acting thus as a 3-connected nodal point (Figure 6). The resulting 2D net is binodal 3- and 6-connected with point (Schläfli) symbol $(4^3)^2(4^6{\cdot}6^6{\cdot}8^3)$ type kgd [the Shubnikov plane net (3.6.3.6)/dual agrees with *TOPOS* program analysis[15]].

dx.doi.org/10.1021/ic300816r | *Inorg. Chem.* 2012, 51, 11349–11355

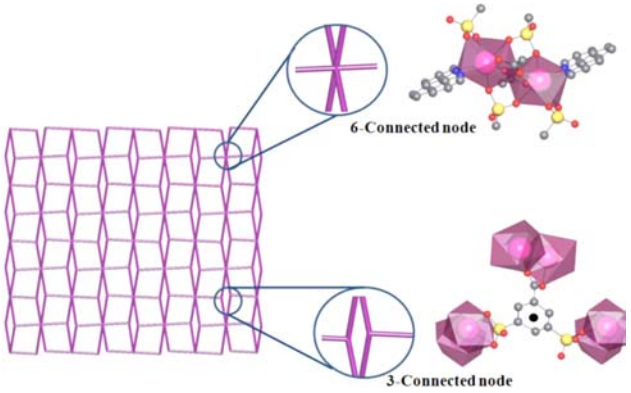

Figure 6. Schematic description of the kgd net $(4^3)^2(4^6{\cdot}6^6{\cdot}8^3)$ topological type viewed in the plane (011) for **RPF-19**.

STRUCTURAL COMPARISON

Three new compounds belonging to two new structural types were hydrothermally synthesized under similar reaction conditions. The difference between these structures can be explained as follows: In **RPF-18**, the framework is formed by (LnO_6N_2)TPRS-8 primary building units (PBUs); the sulfonate and carboxylate groups bridge alternatively ($\eta^2\mu_2$ mode) the PBUs in perpendicular directions, forming chains as SBUs, with Ln−(μ-carboxylate)−Ln = 5.7228(7) and 5.6724(10) Å and Ln−(μ-sulfonate)−Ln = 6.2812(7) and 6.2442(9) Å for Pr and La compounds, respectively.

In **RPF-19**, the PBUs are formed by (LnO_7N_2)TPRS-9 polyhedra. The SBUs come from the linkage of two PBUs via oxo−carboxylate bridges ($\eta^3\mu_2$ mode) in $Ln_2O_{12}N_4$ dimeric clusters with a Nd−Nd distance of 4.2975(5) Å. The carboxylate group is twisted 44.94° with respect to the aromatic ring because of its chelate bridge coordination in the bimetallic cluster, with distances Nd1−(μ-O7)−Nd1 and Nd1−O8 being 2.392(4), 3.077(3), and 2.413(2) Å, respectively.

The sulfonate groups that coordinate in $\eta^2\mu_2$ mode in both structural types present two different conformations: anti−syn[16] in **RPF-18**, where the PBUs are separated polyhedra, and syn−syn in **RPF-19**, where each PBU is half of a dimeric cluster, and thus the metals remain at shorter distances from each other (Figure 7).

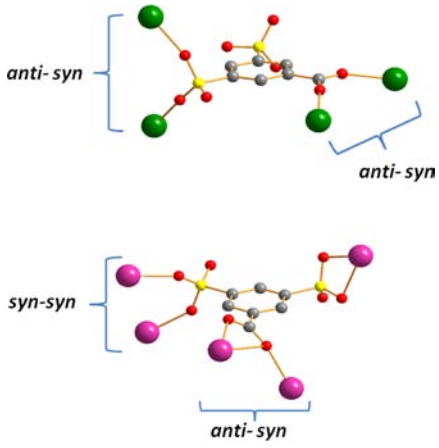

Figure 7. Coordination mode types anti−syn and syn−syn in **RPF-18** and **RPF-19**.

IR Spectra. Although compounds **RPF-18** and **RPF-19** are structurally different, they have similar vibrational spectra. The C−H vibrations belonging to aromatic rings of phenanthroline and 3,5-DSB ligands are found around at ∼3075−3120 and ∼3000−3120 cm^{-1} for **RPF-18** and **-19**, respectively. The bands present at ∼1570 and 1615 cm^{-1} are assigned to ν_{as}(OCO), and the bands at ∼1390 and 1450 cm^{-1} are associated with the symmetric mode for both compounds. S═O and S−O vibrations, observed in the region of ∼1030−1150 cm^{-1}, are related with coordination of the sulfonate group. In this region, we can found four bands characteristic of a bridged bidentate complex ($\eta^2\mu_2$). The double band around ∼410−440 cm^{-1} is assigned to M−O vibrations (Figure S2 in the Supporting Information).

Thermal Study. TGA for the three compounds present thermal stability up to ∼505 °C (Figure S4 in the Supporting Information), where compound decomposition begins with the mass loss corresponding to the organic ligands (**RPF-18-Pr**, calcd 68.5%, found 67.5%; **RPF-18-La**, calcd 66.08%, found 66.0%; **RPF-19-Nd**, calcd 65.54%, found 64.26%) and lanthanide oxysulfate ($Ln_2O_2SO_4$) formation (Figure S5 in the Supporting Information).[17]

Catalytic Study. Cyanohydrins are a very important organic compounds for both synthetic chemistry and biological processes.[18] This organic group is an important stereogenic center precursor of important molecules such as α-hydroxy acids, β-amino alcohols, among other products. In order to obtain cyanohydrin molecules, the use of a catalyst with Lewis acid or base character through which both the substrate and the cyanide precursor are activated is necessary.[18] In this sense, the starting reactives commonly used are aldehydes or ketones with TMSCN as the nucleophilic agent. In this work, we test the activity of the new Ln-MOFs as a heterogeneous catalyst in the aldehyde cyanosylation reaction under solvent-free conditions. First, the materials were tested with benzaldehyde as the standard molecule and varying the amount of catalyst and temperature. The results are summarized in Table 1, and the reaction conditions found were 5% of catalyst, 50 °C, and a N_2 atmosphere (Scheme 2). Comparatively, we found that compound **RPF-19-Nd** presents the highest activity with a TOF value of 12.94 h^{-1} followed by compounds **RPF-18-La** and **RPF-18-Pr** with values of 9.38 and 6.48 h^{-1}, respectively (Figures 8 and 9). In a comparison of the reactivity of our catalyst with that of some previously reported ones (Mn-

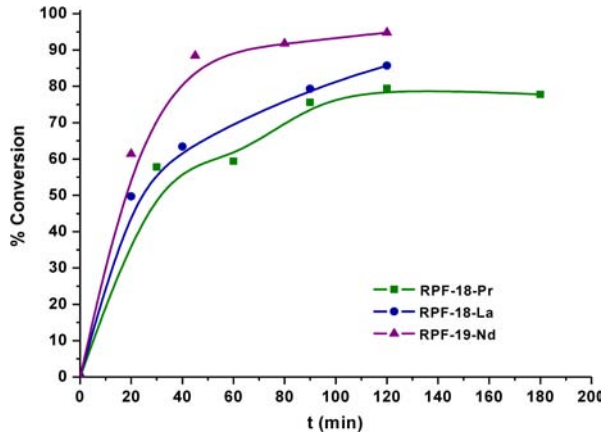

Figure 8. Kinetic profiles for benzaldehyde cyanosilylation for **RPF-18-Pr**, **RPF-18-La**, and **RPF-19-Nd**.

dx.doi.org/10.1021/ic300816r | *Inorg. Chem.* 2012, 51, 11349−11355

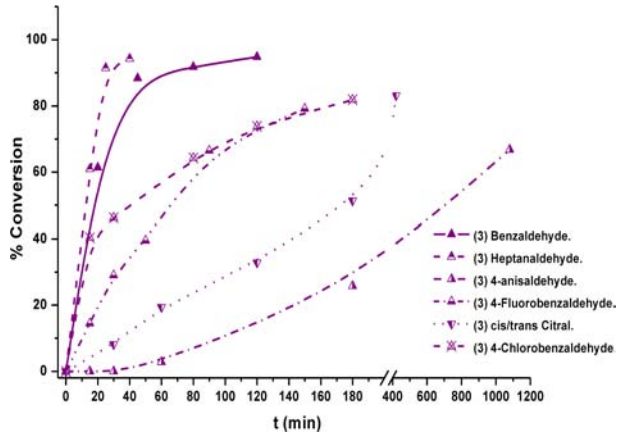

Figure 9. Kinetic profiles for cyanosilylation for different aldehydes for **RPF-19-Nd**.

MOF[19] and Ln-MOF[20]), it was found to be higher than the first (benzaldehyde, 9 h, and yield = 98%), which uses solvent conditions, and slightly less than the second one, which needs an activation treatment and solvent-free conditions to be used (benzaldehyde, 1 h, and yield = 88%).

Once the reactivity of the compounds was determined and upon observation that the **RPF-19** activity is slightly higher than those of the other two, its recyclability was analyzed in order to evaluate its capability as heterogeneous catalysts. In addition, to demonstrate the structure conservation, the catalyst was analyzed by PXRD and did not show any appreciable changes with respect to the patterns obtained before the catalytic reactions (Figure S6 in the Supporting Information).

On the basis of the results reported in Figure 8, we then explored the general utility of the Ln catalysts, performing cyanosilylation of a wide variety of aromatic and aliphatic aldehydes (Table 1). Both of them gave the corresponding cyanohydrin trimethylsilyl ethers in good-to-excellent yields, and distilled products (cyanohydrins) were not formed in any of these cases (Table 2). It seems that the nature of the substituent on the aromatic ring had no dramatic effect on the reaction yield; the lowest yield was obtained for an electron donor group like *p*-methoxybenzaldehyde. The effect of the nature of the aldehyde was evidenced with linear aldehydes as heptanaldehyde and citral; we found that the reactivity follows the order linear > aromatic > citral with high yields (83.2–94.2%) in short-to-medium reaction times (45 min to 7 h).

Reaction with citral does not show any preferential selectivity toward a cis or trans isomer, and the obtained yield is around 50% for each product; this suggests that the catalyst active sites are present on the external surface. The lack of conformational selectivity evidences a clear electronic effect of the substrates in the activity of catalysts.

As is well-known, the lanthanide metals have Lewis acid strength, which is closely related with the ionic radii; in some cases, reactions that involve acid catalysis are well-defined because the reactivity increases with a decrease of the ionic radii.[8,21] In the present case, the reaction is ruled by the Lewis acid character of the catalyst bulk. These can be evidenced in the reactivity found, where the Nd compound is more active than the Pr and La compounds.

Other evidence of the Lewis acid effect on the reactivity in the cyanosilylation reaction was the negative results of the test of other common base-catalyzed reactions like aldol condensation and aldehyde acetalization. With these observations, we can propose that the reaction mechanism involves activation of the carbonyl by the unsaturated metallic center (CN = 8) in **RPF-18-Ln**.

When using **RPF-19-Nd** as the catalyst, an uncoordinated–coordinated equilibrium of the O7 ($\eta^2\mu_2$) in the labile oxo–carboxylate bond [O7–Nd1 = 3.077(3) Å] favors the reaction. Thanks to this equilibrium (C.N = 9 ↔ 8), it is possible to generate a vacant position that has a high Lewis acidity (Scheme 3).

Scheme 3. Possible Mechanism for the Cyanosilylation Reaction in the Case of RPF-18 and RPF-19

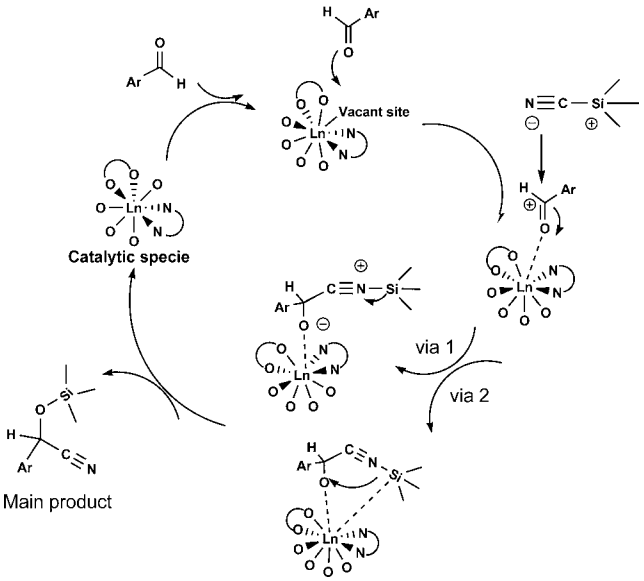

A heterogeneity test was performed for the **RPF-19-Nd** catalyst, using the solid removed from the reaction medium. The catalyst was easily isolated, washed, and reused at least four times without loss of activity (Figure 10). After the last reuse

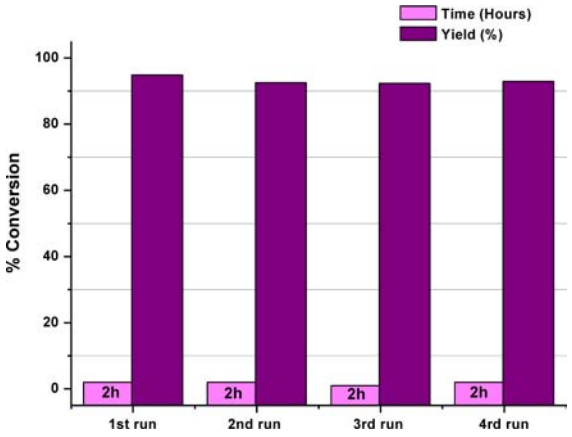

Figure 10. Recyclability of the **RPF-19-Nd** catalyst.

test, a comparison of the final diffraction patterns with the initial ones for each compound showed conservation of the structure and crystallinity, demonstrating that in effect the three new compounds are heterogeneous active catalysts.

In conclusion, we have developed three new MOF materials, which are mild and efficient heterogeneous catalysts for cyanosilylation of various carbonyl compounds. The reported

dx.doi.org/10.1021/ic300816r | *Inorg. Chem.* 2012, 51, 11349–11355

procedure clearly demonstrated that **RPF-19** is an excellent catalyst for the preparation of silyl ethers in relatively short reaction times with low catalyst loading under solvent-free conditions.

These three compounds belong to two 2D structural types, and their nets own different topologies, depending on the multitopic ligand coordination modes.

■ ASSOCIATED CONTENT

Supporting Information

Selected bond lengths and hydrogen bonds and angles, FT-IR spectroscopy, experimental and simulated PXRD patterns, TGA, PXRD patterns after TGA and after catalysis for **RPF-18-Pr**, **RPF-18-La**, and **RPF-19-Nd**. This material is available free of charge via the Internet at http://pubs.acs.org. CCDC reference numbers 873852, 873853, and 873854 contain the supplementary crystallographic data for this paper. These can be obtained, upon request, from the Director, Cambridge Crystallographic Data Centre, 12 Union Road, Cambridge CB2 1EZ, U.K.

■ AUTHOR INFORMATION

Corresponding Author

*E-mail: amonge@icmm.csic.es. Fax: +34913720623.

Notes

The authors declare no competing financial interest.

■ ACKNOWLEDGMENTS

R.F.D. acknowledges a FPI scholarship from the Spanish Ministry of Economy and Competitiveness (MINECO) and Fondo Social Europeo from the EU. This work has been supported by Spanish MCYT Projects MAT2010-17571 and MAT2011-29020-C02-02, Comunidad Autónoma de Madrid (FAMA S2009/MAT-1756), and Consolider-Ingenio (CSD2006-2001).

■ REFERENCES

(1) (a) Qiu, S.; Zhu, G. *Coord. Chem. Rev.* **2009**, *253*, 2891. (b) Snejko, N.; Gutiérrez-Puebla, E.; Martínez, J. L.; Monge, M. A.; Ruiz-Valero, C. *Chem. Mater.* **2002**, *14*, 1879. (c) Gándara, F.; Andrés, A. d.; Gómez-Lor, B.; Gutiérrez-Puebla, E.; Iglesias, M.; Monge, M. A.; Proserpio, D. M.; Snejko, N. *Cryst. Growth Des.* **2008**, *8*, 378. (d) Bernini, M. C.; Gándara, F.; Iglesias, M.; Snejko, N.; Gutiérrez-Puebla, E.; Brusau, E. V.; Narda, G. E.; Monge, M. Á. *Chem.—Eur. J.* **2009**, *15*, 4896. (e) Monge, A.; Gandara, F.; Gutierrez-Puebla, E.; Snejko, N. *CrystEngComm.* **2011**. (f) Fernández-Zapico, E.; Montejo-Bernardo, J. M.; D'Vries, R.; García, J. R.; García-Granda, S.; Rodríguez Fernández, J.; de Pedro, I.; Blanco, J. A. *J. Solid State Chem.* **2011**, *184*, 3289.

(2) (a) Corma, A.; Garcia, H.; Llabrés i Xamena, F. X. *Chem. Rev.* **2010**, *110*, 4606. (b) Dhakshinamoorthy, A.; Alvaro, M.; García, H. *Catal. Sci. Technol.* **2011**, *1*, 856. (c) Lee, J.; Farha, O. K.; Roberts, J.; Scheidt, K. A.; Nguyen, S. T.; Hupp, J. T. *Chem. Soc. Rev.* **2009**, *38*, 1450. (d) Ranocchiari, M.; Bokhoven, J. A. v. *Phys. Chem. Chem. Phys.* **2011**, *13*, 6388. (e) Gomez-Lor, B.; Gutiérrez-Puebla, E.; Iglesias, M.; Monge, M. A.; Ruiz-Valero, C.; Snejko, N. *Inorg. Chem.* **2002**, *41*, 2429. (f) Gándara, F.; Gomez-Lor, B.; Gutiérrez-Puebla, E.; Iglesias, M.; Monge, M. A.; Proserpio, D. M.; Snejko, N. *Chem. Mater.* **2007**, *20*, 72.

(3) Ferey, G. *Chem. Soc. Rev.* **2008**, *37*, 191.

(4) (a) Yoon, M.; Srirambalaji, R.; Kim, K. *Chem. Rev.* **2011**, *112*, 1196. (b) Gandara, F.; Medina, M. E.; Snejko, N.; Gutierrez-Puebla, E.; Proserpio, D. M.; Monge, M. A. *CrystEngComm* **2010**, 12. (c) Platero-Prats, A. E.; Bernini, M. C.; Medina, M. E.; Lopez-Torres, E.; Gutierrez-Puebla, E.; Angeles Monge, M.; Snejko, N. *CrystEngComm* **2011**, *23*, 4965.

(5) Gándara, F.; Puebla, E. G. r.; Iglesias, M.; Proserpio, D. M.; Snejko, N.; Monge, M. A. *Chem. Mater.* **2009**, *21*, 655.

(6) Perles, J.; Iglesias, M.; Ruiz-Valero, C.; Snejko, N. *J. Mater. Chem.* **2004**, *14*, 2683.

(7) Perles, J.; Snejko, N.; Iglesias, M.; Monge, M. A. *J. Mater. Chem.* **2009**, *19*, 6504.

(8) D'Vries, R. F.; Iglesias, M.; Snejko, N.; Alvarez-García, S.; Gutierrez-Puebla, E.; Monge, M. A. *J. Mater. Chem.* **2012**, *22*, 1191.

(9) Gandara, F.; Gomez-Lor, B.; Iglesias, M.; Snejko, N.; Gutierrez-Puebla, E.; Monge, A. *Chem. Commun.* **2009**, 2393.

(10) Côté, A. P.; Shimizu, G. K. H. *Coord. Chem. Rev.* **2003**, *245*, 49.

(11) *SMART*, version 5.04; Bruker-Siemens Inc.: Madison, WI, 1998.

(12) *SAINT*, version 6.28A; Bruker-Siemens Inc.: Madison, WI, 1997.

(13) *SHELXTL*, version 5.1; Bruker-Siemens Inc.: Madison, WI, 1998.

(14) Connelly, N. G.; Damhus, T.; Hartshorn, R. M.; Hutton, A. T. *Nomenclature of Inorganic Chemistry—IUPAC Recommendations 2005*; RSC Publishing: Cambridge, U.K., 2005.

(15) Blatov, V. A.; Scheuchenco, A. P.; *TOPOS*, version 4.0; Samara State University: Russia, 2010.

(16) (a) Cai, J. *Coord. Chem. Rev.* **2004**, *248*, 1061. (b) Sundberg, M. R.; Reijo, S. *Acta Chem. Scand.* **1993**, *47*, 1173.

(17) Zhukov, S. G.; Yatsenko, A.; Chernyshev, V. V.; Trunov, V.; Tserkovnaya, E.; Antson, O.; Hoelsae, J.; Baules, P.; Schenk, H. *Mater. Res. Bull.* **1997**, *32*, 43.

(18) Gregory, R. J. H. *Chem. Rev.* **1999**, *99*, 3649.

(19) Horike, S.; Dincă, M.; Tamaki, K.; Long, J. R. *J. Am. Chem. Soc.* **2008**, *130*, 5854.

(20) Gustafsson, M.; Bartoszewicz, A.; Martín-Matute, B. n.; Sun, J.; Grins, J.; Zhao, T.; Li, Z.; Zhu, G.; Zou, X. *Chem. Mater.* **2010**, *22*, 3316.

(21) (a) Jeong, N. C.; Lee, J. S.; Tae, E. L.; Lee, Y. J.; Yoon, K. B. *Angew. Chem., Int. Ed.* **2008**, *47*, 10128. (b) D'Vries, R. F.; Snejko, N.; Gutiérrez-Puebla, E.; Iglesias, M.; Angeles Monge, M. *Inorg. Chim. Acta* **2012**, *382*, 119.